PHYSICAL REVIEW A **92**, 061602(R) (2015)

Kohn-Sham theory of a rotating dipolar Fermi gas in two dimensions

Francesco Ancilotto
Dipartimento di Fisica e Astronomia "Galileo Galilei" and CNISM, Università di Padova, Via Marzolo 8, 35122 Padova, Italy and CNR-IOM Democritos, Via Bonomea, 265-34136 Trieste, Italy
(Received 31 August 2015; published 10 December 2015)

A two-dimensional dipolar Fermi gas in a harmonic trap under rotation is studied by solving *ab initio* Kohn-Sham equations. The physical parameters used match those of an ultracold gas of fermionic ^{23}Na ^{40}K molecules, a prototypical system of strongly interacting dipolar quantum matter, which was created very recently. We find that, as the critical rotational frequency is approached and the system collapses into the lowest Landau level, an array of tightly packed quantum vortices develops, in spite of the nonsuperfluid character of the system. In this state the system loses axial symmetry and the fermionic cloud boundaries assume an almost perfect square shape. At higher values of the filling factor the vortex lattice disappears, while the system still exhibits square-shaped boundaries. At lower values of the filling factor the fermions become instead localized in a Wigner cluster structure.

DOI: 10.1103/PhysRevA.92.061602 PACS number(s): 03.75.Ss, 73.43.−f

Developments in the field of ultracold dipolar atoms have boosted investigations of many-body effects associated with long-range interactions (see, e.g., the review in Ref. [1]). Recently, the creation of ultracold dipolar gas of fermionic molecules with large intrinsic dipole moments has been achieved [2,3], opening the way to explore the intriguing many-body physics of correlated Fermi systems associated with the long-range anisotropic nature of the dipolar interaction between molecules [4], which includes topological superfluidity [5,6], interlayer pairing between two-dimensional systems, and the formation of dipolar quantum crystals [7].

Two-dimensional (2D) dipolar systems are particularly interesting, since the lifetime of heteronuclear Feshbach molecules with a permanent electric dipole moment increases by the confinement in two dimensions [8]. Indeed, such polar molecules can have very large dipole moments, of the order of 1 D, allowing us to access the regime of strong correlations in a controllable way. A 2D dipolar Fermi liquid, which is stable at low density, is expected to convert into a Wigner crystal at high densities [1,9]. For intermediate values of the interaction strengths, an instability at finite wave vector is predicted, driving the system to a stripe phase [10–12] (see also Ref. [1] and references therein). A recent quantum Monte Carlo study confirmed the liquid-solid transition at high coupling but found that the stripe phase is never energetically favored [13].

A particular fascinating route towards the realization of a strongly correlated system of ultracold gases (either bosonic or fermionic) is the use of rapidly rotating harmonic traps. When the rotational frequency approaches the trap frequency, i.e., just below the limit of centrifugal instability, the single-particle energy spectrum becomes highly degenerate and hence the kinetic energy of the Fermi system is greatly reduced, thus enhancing the role of the interparticle interactions.

A uniform rotation with angular velocity approaching the centrifugal limit is in fact formally equivalent to a magnetic field (in the rotational frame) that regroups single-particle states into discrete, highly degenerate Landau levels (LLs). Such equivalence, for a 2D system, is embodied in the following formal identity [14] involving the many-body Hamiltonian of the (interacting) system in the rotating reference frame:

$$H = \sum_{i=1}^{N}\left(\frac{\mathbf{p}_i^2}{2M} + \frac{M}{2}\omega_h^2 r_i^2 - \Omega\hat{L}_{iz}\right) + V$$
$$= \sum_{i=1}^{N}\left[\frac{1}{2M}(\mathbf{p}_i - M\omega_h \mathbf{e}_z \times \mathbf{r}_i)^2 + \frac{M}{2}\left(\omega_h^2 - \Omega^2\right)r_i^2\right] + V, \quad (1)$$

where V is the interaction energy, Ω is the rotation frequency, and $\hat{L}_{iz}$ is the projection of the angular momentum of the ith particle along the z axis. Here $\mathbf{r}_i = x_i\mathbf{e}_x + y_i\mathbf{e}_y$ is the position vector of the ith particle. When $\Omega = \omega_h$ the noninteracting part reduces to the Landau Hamiltonian of particles with mass M and charge e moving in a constant magnetic field $\mathbf{B} = B\mathbf{e}_z$ of strength $B = 2M\Omega/e$. The eigenvectors of the noninteracting part span Landau levels with energies $\epsilon_n = \hbar\omega_c(n + 1/2)$, where $\omega_c = 2\Omega$.

We consider in the following a two-dimensional spin-polarized dipolar Fermi gas, characterized by an interaction term in Eq. (1) $V = \sum_{i<j}^{N} \frac{d^2}{|\mathbf{r}_i - \mathbf{r}_j|^3}$. Here d is the electric dipole moment of an atom or molecule and $\mathbf{r}, \mathbf{r}'$ are coordinates in the 2D x-y plane. Since the dipole moments are aligned parallel to the z axis, the (long-range) pair potential is purely *repulsive*. The range of the dipole-dipole interaction is characterized by the length $r_0 = Md^2/\hbar^2$.

Exotic forms of vortex lattices, e.g., square, stripe, and bubble crystal lattices, are expected in rotating Bose Einstein condensates when the critical rotational frequency is approached [15–17]. Rotating dipolar Fermi gases have been proposed [18,19] as suitable candidates to realize the Laughlin-like state and more exotic quantum liquids, as well as their crossover behavior to Wigner crystals. At variance with the case of a nonrotating dipolar Fermi gas in a 2D trap, where the crystalline state becomes energetically favored at high densities, in the case of a fast rotating dipolar gas, the situation is reversed [1]: Rotating dipoles in the lowest LL (LLL) behave similarly to electrons, where the crystalline phase is stable at low densities. Indeed, it has been shown [20,21] that a rapidly rotating polarized 2D dipolar Fermi gas undergoes a transition

to a crystalline state, similar to the two-dimensional Wigner electron crystal in a magnetic field, for sufficiently low value of the filling factor $\nu < 1/7$. Here $\nu \equiv 2\pi l^2 n_F$ (where n_F is the areal density of the fermionic system and $l = \sqrt{\hbar/M\omega_h}$ is the magnetic length) gives the fraction of the occupied LLL. At filling factor $\nu = 1/3$ the system is instead well described in terms of fractional quantum Hall-like states [17].

Density-functional theory (DFT), which is perhaps the most widely used and successful technique in electronic structure calculations of condensed matter systems, has only recently entered the field of cold gases as a useful computational tool that goes beyond the mean-field description by taking into account correlation effects and thus is capable of yielding quite accurate results in agreement with more microscopic (but also much more computationally expensive) approaches. The well-known Kohn-Sham (KS) mapping [22] of the many-body problem into a noninteracting one make this approach applicable in practice, often within the so-called local-density approximation (LDA) [22]. Recently, KS DFT was applied to cold atomic Fermi gases in optical lattices [23] and to the study of a unitary trapped Bose gas [24]. Density-functional theory approaches have been used recently to describe a Fermi dipolar system in various single-orbital approximations (Thomas-Fermi [9], Thomas-Fermi-Dirac [25], Thomas-Fermi–von Weizsacker [26,27] approximations). In Ref. [28] a parameter-dependent DFT LDA approach was used to study a small number of harmonically trapped fermions. A somewhat different density-functional formalism, whose applicability is however limited to a small number of particles and which is based on the self-consistent combination of the weak- and the strong-coupling limits, has been proposed to study the ground-state properties of strongly correlated dipolar and ionic ultracold bosonic and fermionic gases [29].

Here we use the conventional KS approach, based on an accurate description for the correlation energy of the dipolar system as provided by diffusion Monte Carlo calculations [13]. Our approach does not require any adjustable parameter and thus belongs to the family of *ab initio* methods well known in the electronic structure community. The Kohn-Sham formulation [22] of density-functional theory [30] for an inhomogeneous system of N interacting particles with mass M is based on the following energy functional of the density that includes the exact kinetic energy of a fictitious noninteracting system and the interaction energy functional $E_{\mathrm{HF}C}$:

$$E_{\mathrm{KS}}[\rho] = -\frac{\hbar^2}{2M}\sum_i \int \phi_i^*(\mathbf{r})\nabla^2\phi_i(\mathbf{r})d\mathbf{r} + E_{\mathrm{HF}C}[\rho]. \quad (2)$$

The $\{\phi_i(\mathbf{r}), i = 1,N\}$ are single-particle orbitals, forming an orthonormal set $\langle\phi_i|\phi_j\rangle = \delta_{ij}$ filled up to the Fermi level. The total density of the system $\rho(\mathbf{r}) = \sum_{i=1}^{N}|\phi_i(\mathbf{r})|^2$ $E_{\mathrm{HF}C}$ is the sum of the direct plus exchange dipolar interaction term (usually termed the Hartree-Fock energy E_{HF}) and the correlation energy E_C. The Hartree-Fock energy of a dipolar Fermi gas in two dimensions has two contributions. The first, for the homogeneous system of the surface density $\rho = N/A$, is

$$E_{\mathrm{HF}}^{(1)} = \frac{256}{45}Nd^2\sqrt{\pi}\rho^{3/2}. \quad (3)$$

The second term is *nonlocal* in nature and is given by [25,26]

$$E_{\mathrm{HF}}^{(2)} = -\pi d^2 \int d\mathbf{r}\,\rho(\mathbf{r}) \int d\mathbf{r}' \int \frac{d\mathbf{k}}{(2\pi)^2} k e^{-i\mathbf{k}\cdot(\mathbf{r}-\mathbf{r}')}\rho(\mathbf{r}'). \quad (4)$$

This term vanishes in the uniform limit, while the negative sign crucially lowers the total energy of the system in inhomogeneous configurations. This term has been shown to be essential to stabilize structures such as one-dimensional stripe phases and the Wigner crystal that is expected at high densities [9]. In the following we will treat $E_{\mathrm{HF}}^{(1)}$ and E_C within the LDA, i.e.,

$$E_{\mathrm{HF}}^{(1)} + E_C = \int \left[\frac{256}{45}d^2\sqrt{\pi}\rho(\mathbf{r})^{5/2} + \rho(\mathbf{r})\epsilon_C(\rho(\mathbf{r}))\right]d\mathbf{r}, \quad (5)$$

where $\epsilon_C(\rho)$ is the correlation energy per particle of the *homogeneous* system of density ρ, as obtained from the (virtually exact) diffusion Monte Carlo calculations of Ref. [13].

The total energy functional in the corotating frame with constant angular velocity Ω (where the dipolar system appears at rest) and in the presence of an isotropic harmonic trapping potential of frequency ω_h, $U(\mathbf{r}) = \frac{1}{2}M\omega_h^2(x^2+y^2)$, is given by

$$E[\rho] = E_{\mathrm{KS}}[\rho] + \int d\mathbf{r}\,\rho(\mathbf{r})U(\mathbf{r}) - \Omega\langle L_z\rangle. \quad (6)$$

Here $\langle L_z\rangle$ is the total angular momentum of the system. Constrained minimization of the above functional leads to the coupled KS eigenvalues equations

$$\left[-\frac{\hbar^2}{2M}\nabla^2 + V_{\mathrm{KS}}\right]\phi_i(\mathbf{r}) = \epsilon_i\phi_n(\mathbf{r}), \quad (7)$$

where

$$V_{\mathrm{KS}}(\mathbf{r}) = \epsilon_C(\rho(\mathbf{r})) + \rho(\mathbf{r})\frac{\partial\epsilon_C}{\partial\rho} + \frac{128}{9}d^2\sqrt{\pi}\rho^{3/2}(\mathbf{r}) - \Omega\hat{L}_z$$
$$-2\pi d^2\int d\mathbf{r}'\int\frac{d\mathbf{k}}{(2\pi)^2}ke^{-i\mathbf{k}\cdot(\mathbf{r}-\mathbf{r}')}\rho(\mathbf{r}') \quad (8)$$

and $L_z = -i\hbar(x\partial/\partial y - y\partial/\partial x)$.

We seek stationary solutions $\{\phi_i(\mathbf{r}), i = 1,N\}$ by propagating in imaginary time the time-dependent version [22] of the KS equations (7). Both the density and the orbitals ϕ_i have been discretized in Cartesian coordinates using a spatial grid fine enough to guarantee well converged values of the total energy. The orthogonality between different orbitals has been enforced by a Gram-Schmidt process. The spatial derivatives entering Eq. (7) have been calculated with accurate 13-point formulas, while fast Fourier techniques have been used to efficiently calculate the nonlocal term entering the KS potential V_{KS}.

We take in our calculations $d = 0.8$ D, which is appropriate to ^{40}K ^{23}Na molecules in the experimental realization of Ref. [3]. The mass is that of a ^{40}K ^{23}Na molecule. The range of the potential is thus $r_0 = Md^2/\hbar^2 \sim 0.6\ \mu\mathrm{m} \sim 0.2a_H$, $a_H = \sqrt{\hbar/2M\omega_h}$ being the oscillator length. In the ground state of the nonrotating system, the adimensional interaction strength characterizing the system is $k_F r_0 \sim 0.9$ (where

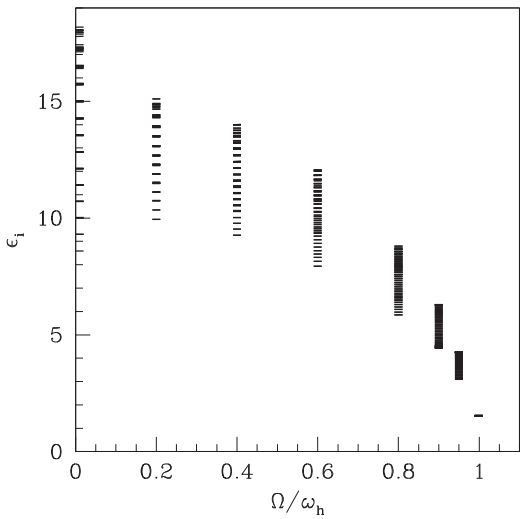

FIG. 1. Calculated KS eigenvalues (in units of $\hbar\omega_h$) for $N = 100$ fermions for different values of the rotational frequency Ω.

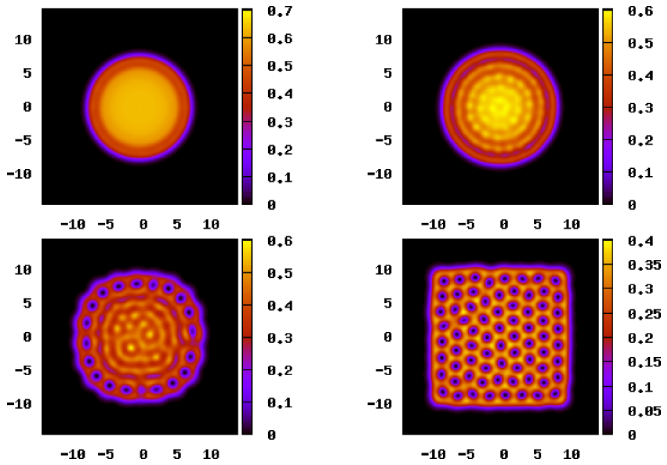

FIG. 2. (Color online) Density of the dipolar system ($N = 100$) at selected values of Ω/ω_h. From left to right and from top to bottom: $\Omega/\omega_h = 0.96, 0.98, 0.99, 0.999$. The x-axis coordinates are in units of a_h, while the density is in units of a_h^{-2}.

$k_F = \sqrt{4\pi\rho_{\max}}$ is the Fermi wave vector of the 2D system at a density equal to the maximum density in the center of the trap), i.e., a relatively weak value that can easily be achieved in experiments. The interparticle distance $\langle r\rangle$ is larger than the range of the interaction, being $\langle r\rangle/r_0 \sim 3.6$. The corresponding dipolar interaction energy $E_d = d^2/\langle r\rangle^3$ approaches 20% of the local Fermi energy $\hbar^2 k_F^2/2M$. In spite of the relatively weak coupling, as a consequence of the rotation, strong correlation effects will show up in the density distribution of the calculated stationary states, as shown in the following. We consider systems with up to $N = 200$ fermions.

We show in Fig. 1 the evolution of the calculated single-particle KS eigenvalues ϵ_i for the case $N = 100$, as the rotational frequency Ω approaches from below the harmonic frequency ω_h. At $\Omega = 0.999\omega_h$ it appears that all the energy levels collapse into a single level, the (highly degenerate) LLL.

It is instructive to follow how the density of the system evolves as Ω is increased. This is shown in Fig. 2, where the densities of selected configurations corresponding to different values of Ω are displayed.

For low values of Ω ($\Omega = 0$ included) the calculated stationary states have circular symmetry and the density has the familiar, almost featureless shape of a trapped cold gas cloud. As soon as Ω approaches ω_h, however, a ring of equally spaced deep dimples develops close to the periphery of the cloud, while the systems loses its axisymmetric shape. Eventually, very close to ω_h, an array of tightly packed vortices develops, similarly to the Abrikosov lattice of vortices in rotating superfluids, while the system boundaries acquire a surprising *square* shape.

The calculated current density in the state with $\Omega/\omega_h = 0.999$ in Fig. 2 appears indeed to be circulating around the zero-density minima (black dots in the bottom right panel of Fig. 2), as expected for a vortex array. The total angular momentum $\langle \hat{L}_z\rangle$ shows also the typical behavior associated with the nucleation of quantum vortices, i.e., a sequence of rounded steps (with amplitudes $\sim N\hbar$) with increasing rotation frequency Ω, as more vortices are nucleated in the system during the minimization process leading to the stationary state shown in the bottom right panel of Fig. 2. The average distance d_v between vortices in the structure shown in Fig. 2 is $\sim$20% larger than the one calculated (assuming a triangular vortex lattice of areal density n_v) using Feynman's formula [31], $n_v = 2/\sqrt{3}d_v^2 = M\Omega/\pi\hbar$.

Quantized vortices in Fermionic cold gases are usually associated with pairing interactions, as in the BCS side of a unitary Fermi gas [32], where they are considered the hallmark of the superfluid character of the system. The presence of vortices in a system with purely repulsive interactions, like the one studied here, has been predicted to occur in fermion systems with purely repulsive interaction such as quantum dots, where the rotation is induced by an external magnetic field (see, for instance, Ref. [33]). Indirect evidence of vortices in ultrasmall fermion droplets ($N = 6$) with aligned dipoles has been provided in Ref. [34]. However, due to the implicit symmetry constraints in the calculations of Ref. [34] multivortex structures like the one shown in Fig. 2 did not show up in the calculated density profiles.

A striking feature of the $N = 100$ system in the LLL is the lack of axial symmetry represented by the unusual square-shaped boundaries [35]. This seems to be intimately connected with the interactions between fermions: The system shown in Fig. 2, under the same conditions but with no interactions between fermions, exhibits density profiles with circular symmetry all the way up to ω_h. Deviations from axisymmetric configurations in isotropic trapping have been found in a fast rotating Bose-Einstein condensate (BEC) at overcritical rotation [36], as a consequence of the interatomic forces. Stable, nonaxisymmetric multilobed shapes also characterize the fast rotation of classical liquid droplets [37]. The symmetry-breaking instability observed in the present work might also be related to the so-called Pomeranchuk instability [38], i.e., a change in the topology of the Fermi surface like the one accompanying, e.g., the first-order transition from the isotropic to the nematic phase in a dipolar gas in an optical lattice [39].

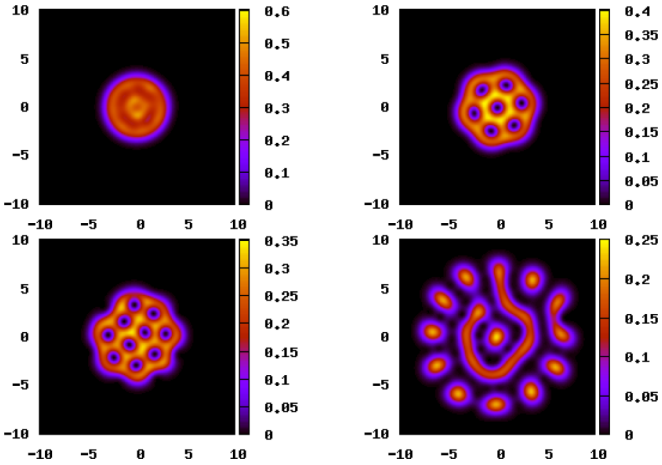

FIG. 3. (Color online) Density of the dipolar system ($N = 13$) at selected values of Ω/ω_h From left to right and from top to bottom: $\Omega/\omega_h = 0.90, 0.96, 0.98, 0.999$. The x-axis coordinates are in units of a_h, while the density is in units of a_h^{-2}.

The configuration shown in the bottom right panel of Fig. 2 corresponds to a filling factor $\nu \sim 0.77$. By decreasing the number of fermions in the trap we can reach lower values of ν. One example is shown in Fig. 3, where $N = 13$. Again, as the centrifugal limit is approached, a stationary configuration with an increasing number of vortices is found: Vortices enter the fermion droplet from the low-density periphery (a mechanism common to BECs [40] and helium-4 [41]). As $\Omega \sim \omega_h$ (bottom right panel in Fig. 3), however, a completely different pattern shows up, resembling a cluster of localized particles (albeit with a partially melted second shell). This configuration is characterized by $\nu \sim 0.18$. We take this as a clear evidence of the formation of a Wigner cluster structure for sufficiently low values of the filling factor.

Higher values of ν can be conversely achieved by increasing the fermions number. In this case the vortex lattice disappears

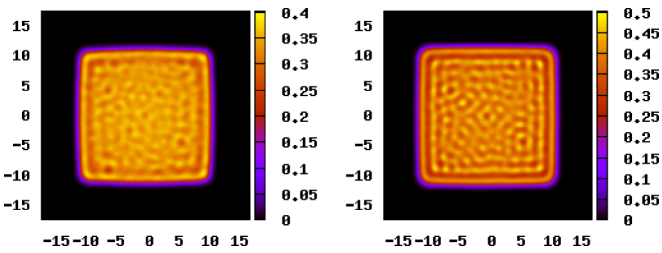

FIG. 4. (Color online) Density of the dipolar system at $\Omega/\omega_h = 0.999$ for $N = 160$ (left) and $N = 200$ (right), corresponding to filling factors $\nu = 1.08$ and 1.25, respectively. The units are the same as in Fig. 3.

and the smoother structures shown in Fig. 4 develop. Here $\nu = 1.08$ and 1.25, respectively (corresponding to $N = 160$ and 200 fermions). Note, however, that the peculiar square-shaped boundaries remain even at higher values of the filling factor.

Although small numbers of cold trapped atoms, like the ones considered here, can nowadays be achieved in experiments [42], we expect that the surprising phenomenology revealed by our calculations should be present also in larger systems of rotating dipolar fermionic molecules in quasi-2D harmonic traps. Achieving rotation frequencies $\Omega \sim 0.999\omega_h$ is a challenging task, but definitely within the reach of current experiments [14]. Due to the relatively high contrast of the vortex array shown in Fig. 2, its observation should be possible by direct imaging of the atomic cloud after expansion (the vortex lattice in quantum dots still awaits experimental detection).

The author thanks S. Giorgini and N. Matveeva for having shared their DMC numerical results and S. Giorgini, L. Salasnich, F. Toigo, J. Boronat, and M. W. Cole for useful discussions and comments.

[1] M. A. Baranov, Phys. Rep. **464**, 71 (2008).
[2] S. Ospelkaus *et al.*, Science **327**, 853 (2010).
[3] J. W. Park, S. A. Will, and M. W. Zwierlein, Phys. Rev. Lett. **114**, 205302 (2015).
[4] M. A. Baranov, M. Dalmonte, G. Pupillo, and P. Zoller, Chem. Rev. **112**, 5012 (2012).
[5] G. M. Bruun and E. Taylor, Phys. Rev. Lett. **101**, 245301 (2008).
[6] N. R. Cooper and G. V. Shlyapnikov, Phys. Rev. Lett. **103**, 155302 (2009); J. Levinsen, N. R. Cooper, and G. V. Shlyapnikov, Phys. Rev. A **84**, 013603 (2011).
[7] L. M. Sieberer and M. A. Baranov, Phys. Rev. A **84**, 063633 (2011).
[8] M. H. G. de Miranda *et al.*, Nat. Phys. **7**, 502 (2011).
[9] B. P. van Zyl, W. Kirkby, and W. Ferguson, Phys. Rev. A **92**, 023614 (2015).
[10] M. M. Parish and F. M. Marchetti, Phys. Rev. Lett. **108**, 145304 (2012).
[11] K. Sun, C. Wu, and S. Das Sarma, Phys. Rev. B **82**, 075105 (2010).
[12] J. K. Block and G. M. Bruun, Phys. Rev. B **90**, 155102 (2014).
[13] N. Matveeva and S. Giorgini, Phys. Rev. Lett. **109**, 200401 (2012).
[14] A. L. Fetter, Rev. Mod. Phys. **81**, 647 (2009).
[15] N. R. Cooper, E. H. Rezayi, and S. H. Simon, Phys. Rev. Lett. **95**, 200402 (2005).
[16] V. Schweikhard, I. Coddington, P. Engels, V. P. Mogendorff, and E. A. Cornell, Phys. Rev. Lett. **92**, 040404 (2004).
[17] M. A. Baranov, K. Osterloh, and M. Lewenstein, Phys. Rev. Lett. **94**, 070404 (2005).
[18] T.-L. Ho and C. V. Ciobanu, Phys. Rev. Lett. **85**, 4648 (2000).
[19] K. Osterloh, N. Barberan, and M. Lewenstein, Phys. Rev. Lett. **99**, 160403 (2007).
[20] M. A. Baranov, H. Fehrmann, and M. Lewenstein, Phys. Rev. Lett. **100**, 200402 (2008).

[21] S.-D. Jheng, T. F. Jiang, and S.-C. Cheng, Phys. Rev. A **88**, 051601(R) (2013).
[22] W. Kohn and L. J. Sham, Phys. Rev. **140**, A1133 (1965).
[23] P. N. Ma, S. Pilati, M. Troyer, and X. Dai, Nat. Phys. **8**, 601 (2012).
[24] M. Rossi, F. Ancilotto, L. Salasnich, and F. Toigo, Eur. Phys. J. **224**, 565 (2015).
[25] B. Fang and B.-G. Englert, Phys. Rev. A **83**, 052517 (2011).
[26] B. P. van Zyl, E. Zaremba, and P. Pisarski, Phys. Rev. A **87**, 043614 (2013).
[27] B. P. van Zyl, A. Farrell, E. Zaremba, J. Towers, P. Pisarski, and D. A. W. Hutchinson, Phys. Rev. A **89**, 022503 (2014).
[28] S. H. Abedinpour, R. Asgari, B. Tanatar, and M. Polini, Ann. Phys. (N.Y.) **340**, 25 (2014); H. Ustunel, S. H. Abedinpour, and B. Tanatar, J. Phys.: Conf. Ser. **568**, 012020 (2014).
[29] F. Malet, A. Mirtschink, C. B. Mendl, J. Bjerlin, E. Ö. Karabulut, S. M. Reimann, and P. Gori-Giori, Phys. Rev. Lett. **115**, 033006 (2015).
[30] P. Hoenberg and W. Kohn, Phys. Rev. **136**, B864 (1964).
[31] R. P. Feynman, in *Progress in Low Temperature Physics*, edited by C. J. Gorter (North-Holland, Amsterdam, 1955), Vol. 1, p. 1.
[32] M. Zwierlein *et al.*, Nature (London) **435**, 1047 (2005).
[33] H. Saarikoski, A. Harju, M. J. Puska, and R. M. Nieminen, Phys. Rev. Lett. **93**, 116802 (2004).
[34] G. Eriksson, J. C. Cremon, M. Manninen, and S. M. Reimann, Phys. Rev. A **86**, 043607 (2012); M. Toreblad, M. Borgh, M. Koskinen, M. Manninen, and S. M. Reimann, Phys. Rev. Lett. **93**, 090407 (2004).
[35] I have checked that the unusual square shape of the system boundaries shown in the bottom right panel of Fig. 2 is not an artifact due to the particular cell or mesh used in the calculations or to the use of periodic boundary conditions: The same configuration is found using a square simulation box with sides 50% larger than the ones shown in the figure or using a rectangular simulation box (with unequal mesh spacing along the x and y directions).
[36] A. Recati, F. Zambelli, and S. Stringari, Phys. Rev. Lett. **86**, 377 (2001).
[37] R. A. Brown and L. E. Scriven, Proc. R. Soc. London Ser. A **371**, 331 (1980).
[38] I. Ia. Pomeranchuk, Sov. Phys. JETP **8**, 361 (1959).
[39] C. Lin, E. Zhao, and W. V. Liu, Phys. Rev. B **81**, 045115 (2010).
[40] D. A. Butts and D. S. Rokhsar, Nature (London) **397**, 327 (1999).
[41] F. Ancilotto, M. Pi, and M. Barranco, Phys. Rev. B **91**, 100503(R) (2015).
[42] F. Serwane, G. Zurn, T. Lompe, T. B. Ottenstein, A. N. Wenz, and S. Jochim, Science **332**, 336 (2011).